華中科技大學

本科生毕业设计（论文）参考文献译文本

译文出处：A Multi-Phase PM Synchronous Generator Torque Control for Direct-Drive Wind Turbines

院　　系 电气与电子工程学院

专业班级 电气 2006 班

姓　　名 徐首彧

学　　号 U202012360

指导教师 叶才勇

译文要求

一、 译文内容须与课题（或专业内容）联系，并需在封面注明详细出处。

二、 出处格式为

图书：作者. 书名. 版本（第×版）. 译者. 出版地：出版者，出版年. 起页～止页

期刊：作者. 文章名称. 期刊名称，年号，卷号（期号）：起页～止页

三、 译文不少于 5000 汉字（或 2 万印刷符）。

四、 翻译内容用五号宋体字编辑，采用 A4 号纸双面打印，封面与封底采用浅蓝色封面纸（卡纸）打印。要求内容明确，语句通顺。

五、 译文及其相应参考文献一起装订，顺序依次为封面、译文、文献。

六、 翻译应在第七学期完成。

译文评阅

导师评语

应根据学校“译文要求”，对学生译文翻译的准确性、翻译数量以及译文的文字表述情况等做具体的评价后，再评分。

译文翻译准确性良好，字数符合要求，文字表述基本流畅。

评分：90（百分制）　　指导教师(签名)：叶才勇

2024 年 1 月 5 日

用于直驱风力涡轮机的多相永磁同步发电机转矩控制

摘要

本文提出了一种使用十二相永磁同步电机的直接驱动风力涡轮机转矩控制算法。为了改善直接驱动风力涡轮机的扭矩控制、发电量和可靠性，本文引入了面向输出四个独立三相星形子系统的电机。为多相电机控制开发了一种特定的坐标变换，允许对每个三相子系统进行独立和解耦管理。本文介绍了所提控制算法的综合和仿真结果。

关键词:多相电机控制；永磁同步发电机；可再生能源；风力发电；直驱式风力涡轮机

1. 前言

双馈感应发电机（DFIG）是风力涡轮机（WT）最广泛使用的机电转换系统。它允许使用连接到转子绕组的电子功率转换器对涡轮机进行变速控制，额定功率等于或小于大约 30%的电机功率。根据年发电量-总成本比进行的大量经济分析表明，DFIG 风机是最佳的折中方案。此外，这些涡轮机是最轻便、最经济的，这也是它们在商业 WT 中得到最广泛应用的原因之一[1]。另一方面，在选择风力发电机时，成本并不是唯一需要考虑的因素。尤其是在海上应用中，可靠性和可用性变得越来越重要。在此框架下，齿轮箱是最关键的部件之一[2]。此外，由于需要提高电压故障穿越能力、并网电能质量要求和效率，目前正朝着一种新的过渡方式发展：直接驱动风力涡轮机(DDWT)或带有单级齿轮箱的混合解决方案[3][4]。

DDWT 的特点是叶片轴与发电机直接连接，并使用全尺寸前端变流器。由于避免了齿轮箱的使用，直接驱动结构既减少了主转换系统的损耗，又降低了维护要求，而且由于采用了全尺寸变流器并网接口，还克服了电网故障和电压骤降造成的电压干扰问题。然而，低速大扭矩发电机和全额定前端逆变器的使用使这些风力涡轮机更加昂贵[1][3]。

文献中提出了许多使用不同类型电机的 DDWT。永磁同步电机、感应电机和开关磁阻电机之间的比较表明，对于给定的额定扭矩，永磁同步电机使用的有源材料质量较低，因此适用于大功率应用[5]。

本文研究了带有分布式定子绕组的径向磁通表面安装永磁发电机。特别是分析了以内部定子配置为特征的多相配置。

选择多相 DDWT 的主要原因是可以在更多相之间分配功率和电流，从而降低每相逆变器的额定功率。此外，即使在相位和/或逆变器出现故障时，这种配置也能保证 WT 工作的连续性。因此，在 DDWT 中使用多相电机可提高可靠性，延长工作时间，从而提高年发电量，降低生产和维护成本[2][10][16]。

此外，多相发电机的多功能性还允许：由于其固有的更高自由度，可以更灵活地管理 WT

功率的生产和分配；减少定子 MMF 和 PM 磁场空间谐波相互作用产生的转矩纹波分量；提高效率；由于频率降低，减少直流侧电压纹波的影响。此外，如果相数为奇数，则可以通过定子电流谐波注入来增强转矩产生。在单中性点的不对称六相电机中，这一特性可扩展到偶数相[10][11]。目前，由于电机设计的限制，多相永磁电机在 DDWT 中的应用仅限于小功率应用。事实上，由于要降低轴速，DDWT 的磁极对数特别多。因此，由多相绕组分布引起的极距尺寸增大，在相数较多的情况下，可能会导致电机转子尺寸过度增大。

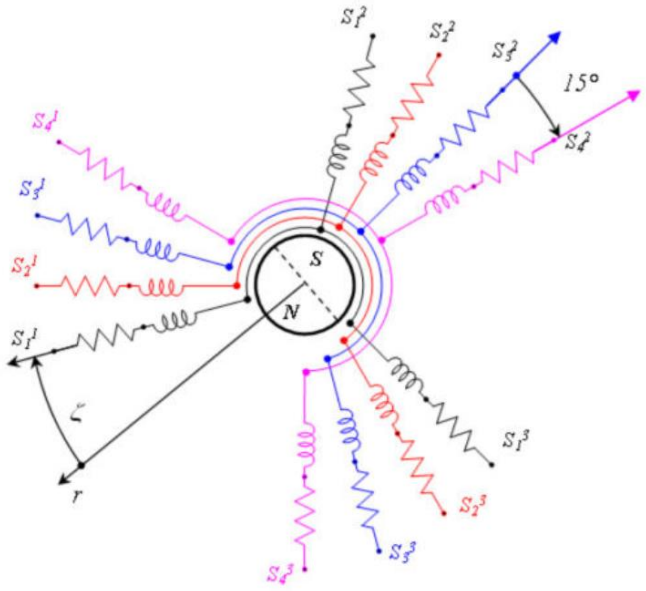

图 1-1 DDWT 永磁同步发电机机械结构示意图

以多相集中绕组和分数槽平衡绕组为特征的交流电机的发展，克服了上述设计上的一些限制，使低速 WT 多相永磁电机得以实现[7][8][12]。

另一方面，多相分式槽电机仍被视为特殊设备，其推广和运行经验有限，无法快速、大规模地应用于大功率分布式绕组多相电机。因此，我们认为，与大功率分布式绕组多相电机制造经验相关的可靠性将在确定两种技术的过渡时间方面发挥重要作用。

本文研究了十二相永磁发电机在 DDWT 应用中的应用，该发电机由四个带隔离中性点的三星形分布式全距绕组组成。特别是，为了提高风能转换过程的可靠性和效率，本文提出了一种控制算法的建模和开发方法，允许对四个电气子系统进行独立和解耦管理。

2. 多相 PM 发电机风力涡轮机结构

目前，WT 的参考额定功率为 3 兆瓦。DDWT 永磁发电机设计的出发点是频率规格，因为使用大量磁极会影响电机的主要尺寸[6]。参照典型的 3MWWT 参数，极对数 p 设为 150。

为了在四个相同的电力系统之间分配风能生产，永磁同步发电机的多星配置被设定为系统设计的一个约束条件。然而，如果相数 m 是偶数质数或奇数，定子绕组的分布就可能不

对称。

在奇数定子绕组三相子系统的情况下，两个连续绕组子系统之间的空间位移可以是$\alpha=\pi/m$。

在六相不对称分布式机器被划分为两个三相子系统的情况下，这种配置的主要优点是，从机电角度来看，它表现为十二相对称分布式永磁机器[10][12]。

根据上述设计限制，参照[1][3]报道的初步电机设计程序，定义了十二相不对称分布式永磁同步发电机。多相发电机的参数见表 I。图 1 是十二相不对称分布式永磁发电机的单极对原理图。

图 2 展示了拟议的 DDWT 配置示意图。每个三相子系统都与额定直流电压为 $2kV$、额定功率为 $750kVA$ *的*交直流电流控制变流器相连，并与浮点电容器组相连。

这种配置非常简单可靠，因为它省去了故障率较高的齿轮箱。此外，DDWT 中最关键的部件之一—电子功率转换器已被四个较小的部件所取代。这种设计提高了可靠性和灵活性，同时降低了 WT 的成本。此外，通过适当控制 WT 叶片俯仰角，即使在 WT 名义速度下出现一个逆变器故障，系统也能继续运行。

由于采用直流输出，这种电气配置特别适合海上应用。这样就可以通过特定的风电场配电配置和合适的直流/直流转换系统，为配电和输电选择合适的直流电压等级[13]。

表 2-1 12 相 PMSG 参数

额定功率	P_n	[MW]	3
额定电压	V_n	[kV]	1.5
相数	m		12
极对数	p		150
定子直径	D	[m]	6
气隙	δ	[mm]	6
120℃下铜线电阻	ρ_m	[μΩm]	0.025
相电感	L_m	[mH]	4
相电阻	R_s	[mΩ]	25-

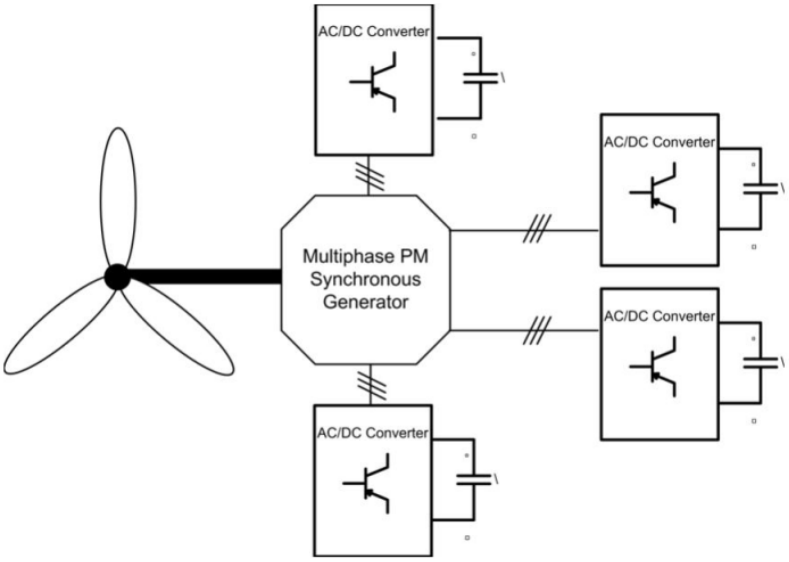

图 2-1 用于十二相永磁同步发电机电源管理的 DDWT 电路图

3. PM 多相发电机的数学模型

为了开发控制系统，我们建立了十二相非对称永磁同步电机的动态数学模型。模型中没有考虑饱和效应、突出效应、时间温度参数依赖性和齿槽转矩。永磁气隙磁通密度的绕组结构和非正弦空间分布应建议开发一种考虑到高空间谐波分量影响的建模程序。然而，专门用于减少转矩谐波纹波影响的多相永磁机优化设计程序允许使用第一次空间谐波分量，这足以详尽地表示多相机的动态机电行为[14]。

一般用于非对称多相机的变换矩阵是基于 Clarke 或 Park 变换矩阵的一般化。

定子参考框架下的定子电压 vs、电流 is 和定子磁通 λs 向量由式（1）中的 12 个分量向量表示，其中下标代表相位，顶点代表各自的三相子系统指数。

采用这种形式化方法，定子电压方程的形式如公式(2)所示，其中 *Rs* 是相位定子电阻，I_{12} 是十二阶同位矩阵。

$$\bar{v}^s = \left[v_a^1, v_b^1, v_c^1, \cdots v_a^k, v_b^k, v_c^k \cdots v_a^4, v_b^4, v_c^4\right]^T$$
$$\bar{i}^s = \left[i_a^1, i_b^1, i_c^1, \cdots i_a^k, i_b^k, i_c^k \cdots i_a^4, i_b^4, i_c^4\right]^T$$
$$\bar{\lambda}^s = \left[\lambda_a^1, \lambda_b^1, \lambda_c^1, \cdots \lambda_a^k, \lambda_b^k, \lambda_c^k \cdots \lambda_a^4, \lambda_b^4, \lambda_c^4\right]^T$$

参照图 1 用 *n* 表示三相子系统的数量，*f 表示*每个子系统的相数（*a*=1，*b*=2，*c*=3），*ϑ 表示*永磁转子磁通矢量参考框架相对于定子的瞬时电角度位置；定子磁通矢量分量 λ_{kf} 可由式（3）表示，其中 λ_m 为与转子永磁体相关的单相磁通的最大值，β_k 为所考虑相位相对于参考相位的电位移角。

$$\bar{v}^s = R_s \mathbf{I}^{12} \cdot \bar{i}^s + \frac{d\bar{\lambda}^s}{dt}$$

Lsf-kj 是定子相电感互感和自感的一般表示方法，其值用公式(4)表示，其中 *s* 是比例 *j/n* 的上一个自然整数。元素 *Lij* 是多相电机电感矩阵 L 的分量。最后两个方程描述了十二个电路之间的磁耦合，在本模型中具有特殊意义。

在公式（5）中报告了十二相非对称空间分布式永磁发电机的帕克变换 **P**，用于获得分析的十二相永磁发电机的 *dqo* 表示。

$$\lambda_f^k = \sum_{j=1}^{m} L_{f+k-1,j}^s \cdot i_j^s + \lambda_m e^{j\left(\vartheta + \beta_f^k\right)}$$

$$L_{i,j}^s = L_{dm} \cdot \cos\left[\frac{\pi}{m}(j-1) + \frac{\pi}{3}(s-1) - \frac{\pi}{m}(i-1)\right] +$$

$$+ L_{sd}\delta_{i,j}; \quad s = SI\left(\frac{j}{n}\right)$$

对公式(2)应用 Park 变换 **P** 可以将每个三相子系统表示在 *dqo* 参考框架中；在这种情况下，电机模型的形式如公式(6)所示。

$$P = \kappa\left[p_{i,j}\right]^{12X12} =$$

$$= \begin{cases} p_{k,nf+c} & = \cos\left[\vartheta + f\frac{2\pi}{3} + \frac{\pi}{3\cdot n}(k-1)\right] \\ p_{n+k,nf+k} & = \sin\left[\vartheta + f\frac{2\pi}{3} + \frac{\pi}{3\cdot n}(k-1)\right] \\ p_{2n+k,nf+k} & = \frac{1}{2} \\ 0 \text{ elsewhere} & k \in [1 \cdots n] \end{cases}$$

Park 应用于电感矩阵 L 的结果见公式（7）。

$$\bar{v}_{dqo}^k = R_s \bar{i}_{dqo}^k + j\omega_r \bar{\lambda}_{dqo}^k + \frac{d\bar{\lambda}_{dqo}^k}{dt}$$

特别是，当绕组连接成 *n* 个具有隔离中性点的三相子系统时，零序分量可被忽略，从而减少了方程和变量的数量[10]。此外，在线性运行条件的假设下，每个三相子系统都可以用 *d-q* 轴来描述，多相机模型可以由一组 *d-q* 方程得到，其中转矩由每个三相子系统贡献之和给出[9][10]。

$$\mathbf{L}_{dqo} = \begin{bmatrix} \left[L_d\right]^{4\times4} & [0]^{4\times4} & [0]^{4\times4} \\ [0]^{4\times4} & \left[L_q\right]^{4\times4} & [0]^{4\times4} \\ [0]^{4\times4} & [0]^{4\times4} & \left[L_o\right]^{4\times4} \end{bmatrix}$$

本文采用了这种模型方法。特别是，由于电机具有磁各向同性的特点，Lq 的值等于 Ld。在永磁转子磁通矢量参考系中，定子磁通矢量 λkdq 可用公式（8）表示。

$$\bar{\lambda}_{dq}^{k} = \lambda_m + \frac{3}{2} L_m \sum_{j=1}^{4} \bar{i}_{dq}^{j} + L_{ls} \bar{i}_{dq}^{k}$$

第 k 个子系统的 dq 电压方程也可以参考基频，用公式(9)中的形式表示。

$$\bar{v}_{dq}^{k} = R\mathbf{I}^2 \bar{i}_{dq}^{k} + \jmath \frac{\omega_r}{\omega_b} \bar{\psi}_{dq}^{k} + \frac{1}{\omega_b} \frac{d\bar{\psi}_{dq}^{k}}{dt}$$

其中，每秒磁通量 ψkdq 与电流矢量之间的关系如式（10）所示，Xm 和 Xls 分别为基频的联动电抗和漏抗。

第 k 个子系统的每秒通量矢量 ψkdq 表明，经过帕克变换后，十二相永磁发电机的数学模型也相当复杂。

$$\bar{v}^{k} = R\bar{i}^{k} + j\frac{\omega_r}{\omega_b}\left[\psi_m + \frac{3}{2} X_m \sum_{j=1}^{n} \bar{i}^{j} + X_{ls} \bar{i}^{-k}\right] + \\ + \frac{3}{2}\frac{X_m}{\omega_b} \sum_{j=1}^{n} \frac{d\bar{i}^{j}}{dt} + \frac{X_{ls}}{\omega_b} \frac{d\bar{i}^{-k}}{dt}$$

此外，第 k 个三相系统的空间矢量电压方程（式（11））突出显示了所有子系统之间的耦合，这给电流矢量控制合成的经典线性化程序的应用带来了高度的复杂性。

根据数学模型，这类电机的扭矩方程如公式（12）所示。

$$T_e = p\lambda_m \sum_{j=1}^{n} i_q^{j} = p\frac{\psi_m}{\omega_b} \sum_{j=1}^{n} i_q^{j}$$

4. PM 多相发电机的解耦控制

为了确定一种变换，使电流矢量控制的合成和实施的经典方法能够扩展到多相永磁电机，我们对系统进行了全面的数学描述。通过使用定子电压 v˙、定子电流˙i 和永磁磁通感应电压 Ψ˙M 的复数元素，引入了复数矢量表示法：

利用上述数据并参考公式(11)，多相永磁发电机的电压方程可以用下面的形式表示：

复矩阵 A˙可以分解为 A˙ls 和 A˙m。A˙ls 是 n×n 的复对角矩阵，其特征是所有元素都等于 a˙ls，其表达式如下：

$$\begin{aligned} \bar{\mathbf{v}} &= \left[\bar{v}_1 \ \ldots \ \bar{v}_n\right]^T \\ \bar{\mathbf{i}} &= \left[\bar{i}_1 \ \ldots \ \bar{i}_n\right]^T \\ \dot{\bar{\Psi}}_M &= \left[j\frac{\omega_r}{\omega_b}\bar{\psi}_m \ \cdots \ j\frac{\omega_r}{\omega_b}\bar{\psi}_m\right]^T \end{aligned}$$

其中$\wp$表示时间导数算子。A˙m 是一个 n×n 的复方阵，其特征是所有元素都等于公式（16）中的 am。

应用乔丹分解法可以实现空间变换，进而实现 A˙矩阵对角化。公式（17）所报告的结果是永磁多相电机新模型的定义，该模型允许明确定义执行解耦和前馈动作的术语。事实上，通过引入关系式（18）中描述的模型，可以获得简化和解耦多相永磁发电机控制的空间变换。考虑到公式（17）中的矩阵 Q 及其逆矩阵：

$$Q=\begin{bmatrix}1 & 1 & 0 & 0\\ 1 & 0 & 1 & 0\\ 1 & 0 & 0 & 1\\ 1 & -1 & -1 & -1\end{bmatrix}$$

并引入以下变换：

$$\begin{aligned}\bar{\mathbf{v}}_J &= Q^{-1}\bar{\mathbf{v}}\\ \bar{\mathbf{i}}_J &= Q^{-1}\bar{\mathbf{i}}\\ \dot{\bar{\Psi}}_{MJ} &= Q^{-1}\dot{\bar{\Psi}}_M\end{aligned}$$

电压方程的形式如公式（19）所示

$$\bar{\mathbf{v}}_J = Q^{-1}\dot{A}Q\bar{\mathbf{i}}_J + \dot{\bar{\Psi}}_{MJ} = \dot{D}\bar{\mathbf{i}}_J + \dot{\bar{\Psi}}_{MJ}$$

其中 D˙是一个复数对角矩阵，可分为实部和虚部，分别用 D˙1 和 D˙2 表示。Ψ˙MJ 的形式如公式（20）所示

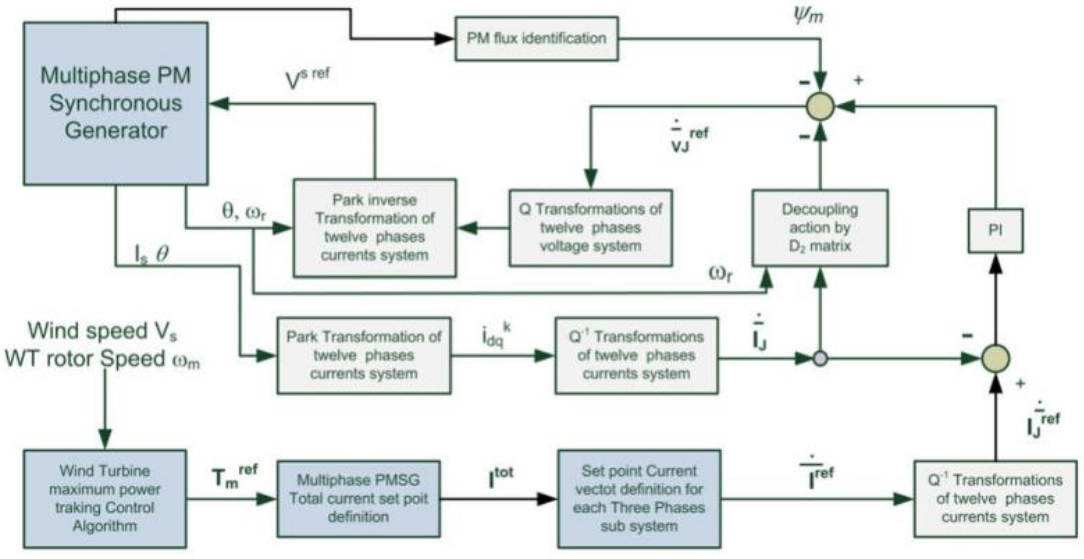

图 4-1 拟议的 DDWT 控制方案框图

$$\dot{\bar{\Psi}}_{MJ}=\left[J\frac{\omega_r}{\omega_b}\bar{\psi}_m 0\cdots 0\right]^T$$

利用所提出的变换，可以简化十二相永磁电机的模型，将四个矢量方程变换为一种形式，从而清晰、轻松地定义运动去耦项，永磁感应电压仅应用于四个等效电路中的第一个，因此，

如果永磁磁通感应电压已知，则可以通过前馈作用直接抵消。所提出的变换被用于开发定子电流矢量控制。

A.电流控制

为了实现转矩控制，对每个三相系统都实施了定子电流矢量控制。参照公式(19)，电流方程可以用公式(21)中的典型形式表示

$$\dot{\bar{x}} = A\bar{x} + B\bar{u}$$

其中 $\bar{x} = \bar{\mathbf{i}}_J$。利用这种表示方法，可以直接证明前馈和解耦控制作用，并通过实施内部模式控制合成 PI 电流环控制器[15]。机器整体的电流控制方案如图 3 所示，第一个环路的 PI 参数指的是 D˙1 矩阵的第一行元素，其值如式（22）所示

$$k_P^1 = \alpha_c \frac{X'}{\omega_b}$$
$$k_I^1 = \alpha_c R$$

其中，X′=6Xm+Xls，其他值见公式（23）。

$$k_P = \alpha_c \frac{X_{ls}}{\omega_b}$$
$$k_I = \alpha_c R$$

其中，αc 是电流环的理想闭环带宽。

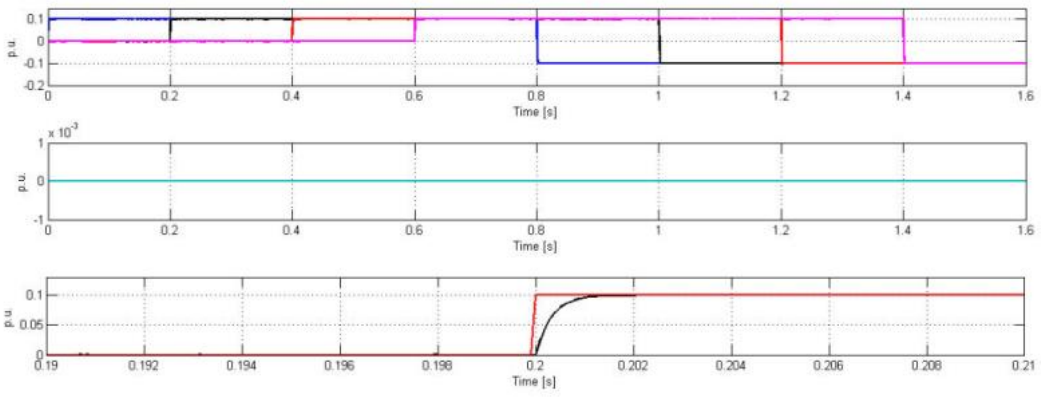

a) iq 时变 b) id 时变 c) 瞬态下 iq 切换点放大图

图 4-2

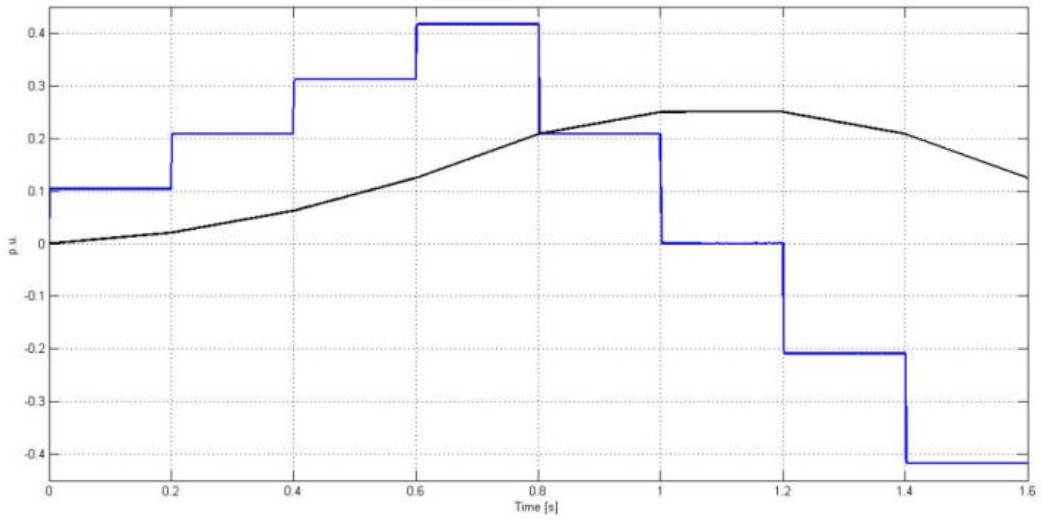

图 4-3 存在 PM 正弦电磁场时的扭矩转速时间演变

B.拟议多相电流控制的仿真结果

使用 Matlab-Simulink 软件模拟了 *3MW* 十二相永磁同步电机的电流控制。电机的主要参数见表 I。PI 电流环控制器的合成带宽为 500*Hz*。为了评估所提出的控制算法的性能，首先对永磁同步电机进行了仿真，假设气隙永磁磁场为正弦空间分布，每个电气子系统以 200 *毫秒的*时间间隔顺序连接，每个子系统的 i_q 步设定点为 0.1p.u。对每个子系统的扭矩设定点进行了反转，目的是验证每个子系统可以进行独立的扭矩控制。

图 4 显示了每个子系统中参考电流和实际 i_q 及 i_d 电流的时间变化。对第二个子系统 i_q 瞬态电流演变的放大显示了实际带宽与设计带宽之间的良好匹配。此外，对 i_d 分量的分析凸显了建议的坐标变换所产生的良好解耦作用，并指出不同子系统的 d 和 q 分量之间不存在相互作用。

图 5 显示了与 i_q 组件变化相对应的扭矩和速度时间变化。

为了分析更高的空间谐波永磁场分布的影响，我们对能够在额定转速下产生相位反电势波形（如图 6 所示）的永磁空间配置进行了建模，并使用该配置进行了与上述相同的模拟。

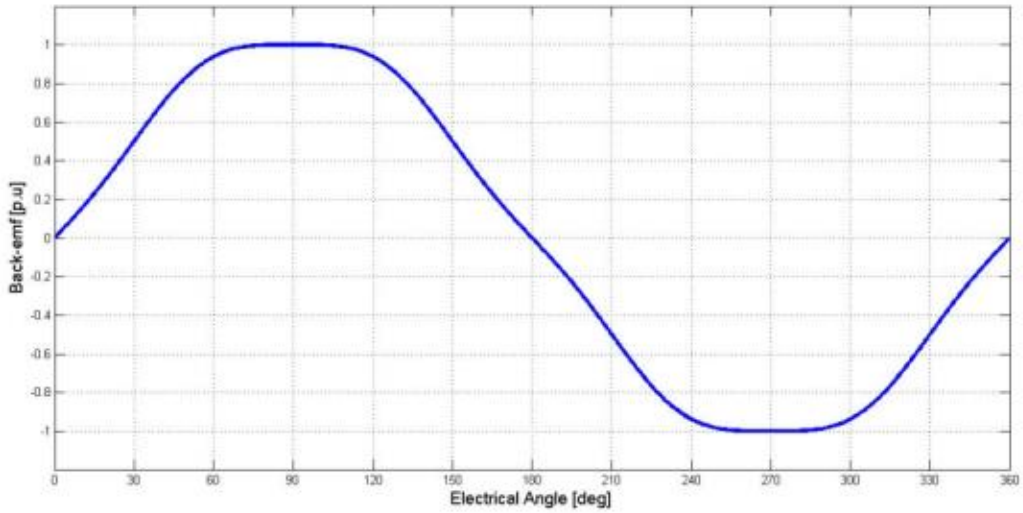

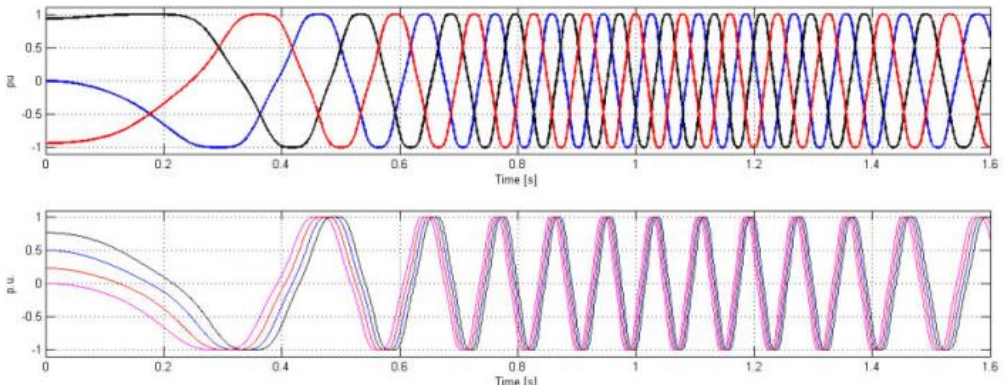

结果见图 7 至图 11。

图 7 显示了永磁通量在第一个子系统和每个子系统第一阶段的时间演变情况。如图 8 所示，五次空间谐波的影响决定了永磁通量中更高次谐波的存在，从而决定了其 d 和 q 分量在每个子系统中的波动。从图 11 中可以观察到永磁高次谐波的主要影响，当馈电的子系统数量为奇数时，会出现扭矩波纹。相反，当供电子系统位移 30 度时，扭矩纹波为零，这与科学文献[12]中报道的此类多相机的结果相吻合。图 8 所示的 i_q 和 i_d 电流的时间变化，以及图 10 所示的每个子系统第一相交流定子电流的时间变化表明，所提出的控制算法在永磁机非正弦空间分布的情况下也能保证解耦作用。

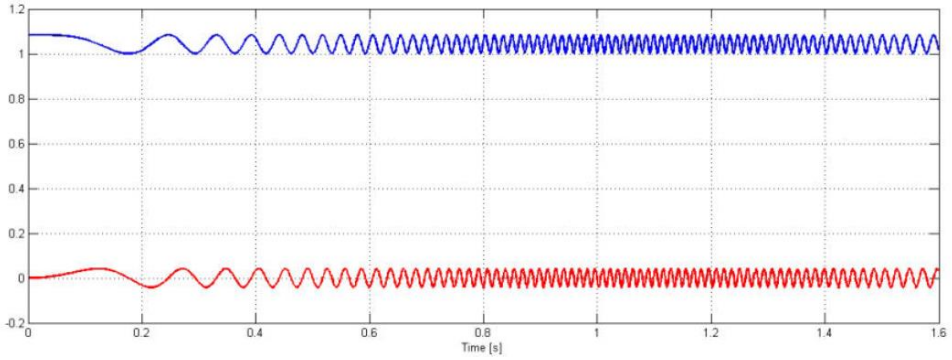

图 4-4 在第一个子平面中的永磁体磁链的 dq 时域解耦

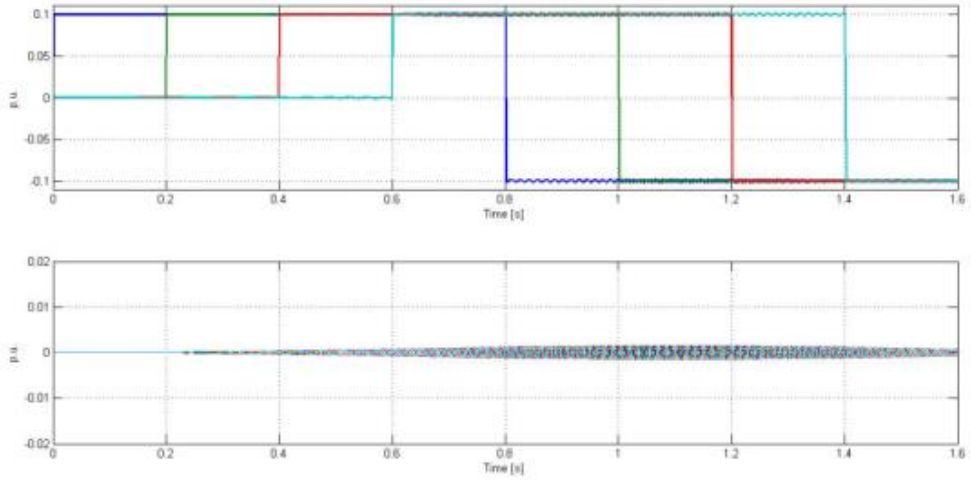

a) q 平面上的定子电流时变 b)q 平面上的定子电流时变

图 4-5

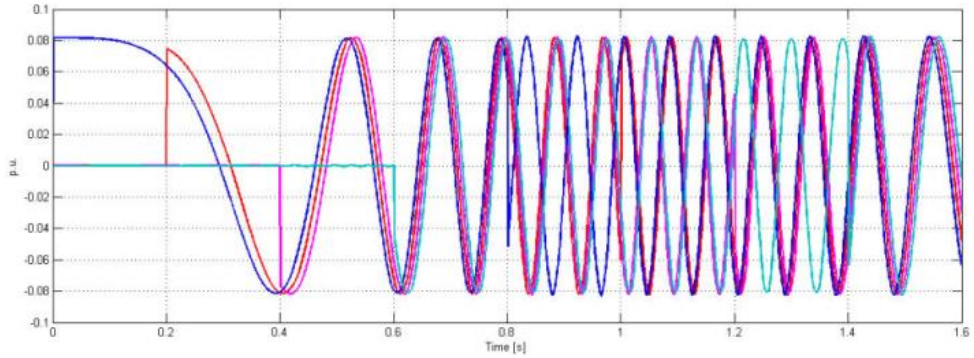

图 4-6 多相永磁电机每个子平面的定子电流

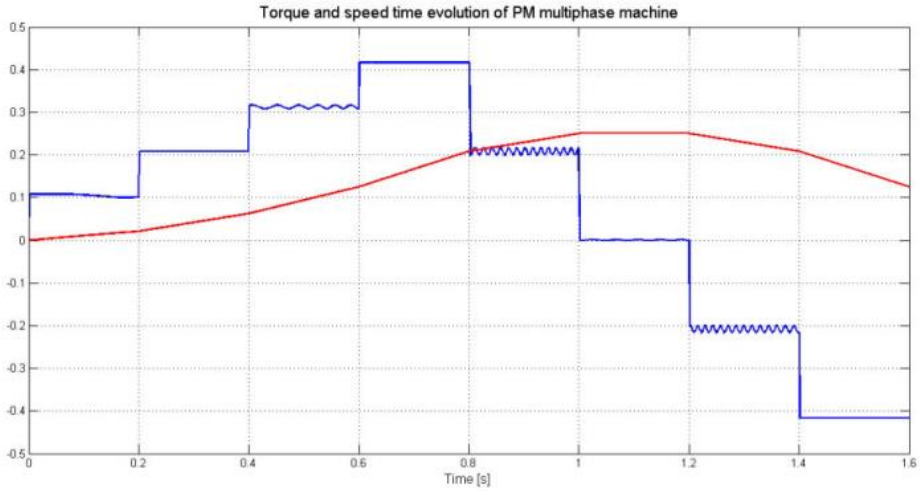

图 4-7 存在非正弦 PM EMF 时的扭矩速度时间演变

模拟结果凸显了所取得的改进，并证实了在 DDWT 应用中使用这种控制配置的可能性。事实上，减少扭矩纹波的可能性是降低扭矩纹波对叶片和风机机械系统产生的结构机械应力影响的重要因素。

5. 结论

本文提出了一种用于直接驱动风力涡轮机的十二相永磁同步电机。特别是为多相电气系统引入了一种新颖的特定坐标变换，以开发一种专用于多相应用的转矩控制算法，其特点是独立的解耦电流控制。报告还介绍了拟议控制算法的综合和数学建模。针对正弦和非正弦永磁感应分布进行了模拟。获得的结果凸显了拟议控制技术的有效性。

参考文献

[1] H. Polinder, F. F. A. van der Pijl, G. de Vilder, and P. J. Tavner, “Comparison of Direct-Drive and Geared Generator Concepts for Wind Turbines”, IEEE Trans. on Energy Conversion, Vol. 21, NO. 3, September 2006

[2] J. Ribrant and L. M. Bertling, “Survey of Failures in Wind Power Systems With Focus on Swedish Wind Power Plants During 1997-2005” IEEE Trans. on Energy Conversion, Vol. 22, No. 1, March 2007

[3] Yu-Shi Xue, Li Han, Hui Li, Li-Dan Xie; “Optimal Design and Comparison of Different PM Synchronous Generator Systems for Wind Turbines” Proc. of International Conference on Electrical Machines and SystemsICEMS 2008 Wuhan, China, 17-20 Oct. 2008, Page(s): 2448 - 2453

[4] Z. Chen, and E. Spooner, Senior Member, “IEEE Grid Power Quality with Variable Speed Wind Turbines”, IEEE Trans. on Energy Conversion, Vol.16, n.2, June 2001

[5] M. R. J. Dubois, “Optimized Permanent Magnet Generator Topologies for Direct-Drive Wind

Turbines" Ph.D. dissertation, Technische Universiteit Delft, Netherland, 2004

[6] Yicheng Chen, P. Pillay, A. Khan; "PM wind generator topologies" IEEE Trans. on Ind. Appl., Volume: 41 , Issue: 6 Year: 2005 , pp:1619 - 1626.

[7] A.M. EL-Refaie,"Fractional-Slot Concentrated-Windings Synchronous Permanent Magnet Machines: Opportunities and Challenges" IEEE Trans.Ind. Electr., vol.57, n.1, Jan. 2010

[8] D. Vizireanu, S. Brisset, and P. Brochet, "Design and optimization of a 9-phase axial-flux PMsynchronous generator with concentrated winding for direct-drive wind turbine",Proc. of IEEE IAS Annu. Meeting, Tampa, FL, 2006, pp.1912-1918.

[9] T. A. Lipo, "A d-q model for six phase induction machines",Proc. Int. Conf. Electrical Machines (ICEM), Athens, Greece, 1980, pp. 860-867.

[10] E. Levi, "Multiphase Electric Machines for Variable-Speed Applications" IEEE Trans. Ind. Electr., Vol.55, n. 5, may 2008.

[11] X. Kestelyn, E. Semail, "A vectorial Approach for Generation of Optimal Current Refernce for Multiphase Permanent Magnet Syncrhronous MAchines in Real Time" IEEE Trans. Ind. Electr. vol.58,n.11 nov. 2011, pp:5057-5065

[12] E. Semail, F. Scuiller, J.F. Charpentier, "Charpentier Multi-star multiphase winding for a high power naval propulsion machine with low ripple torques and high fault tolerant ability". Proc. IEEE Conference on Vehicle Power and Propulsion (VPPC), Year: 2010 , Page(s): 1 - 5

[13] C. Meyer, M. Hoing, A. Peterson, R. W. De Doncker, "Control and Design of DC Grids for Offshore Wind Farms", IEEE Trans.on Ind. Appl., Vol. 43, no. 6, pp. 1475-1482 November/December 2007.

[14] J. Figueroa, J. Coros, F. Viarogue, "Generalised Transformation for Polyphase Phase MOdulation Motors" IEEE Trans. on Energy Conversion vol.21, n.2, June 2006, pp. 332-341.

[15] L. Harnefors, H. P. Nee, "Model-based current control of AC machines using the interna model control method", IEEE Trans. Ind. Appl. vol.34,n.1 pp.133-141, Jan.-Feb 1998

[16] D. Vizireanu, S. Brisset, X. Kestelyn, P. Borchet, Y. Milet, and D. Laloy, "Investigation on multi-star structures for large power direct-drive wind generator", IEEE Trans. Electr. Power Compon. Syst., vol. 35, no. 2, pp.135-152, 2007

2012
International Symposium on Power Electronics,
Electrical Drives, Automation and Motion

A Multi-Phase PM Synchronous Generator Torque Control for Direct-Drive Wind Turbines

Alfonso Damiano, Gianluca Gatto, Ignazio Marongiu, Alessandro Serpi
Universitá di Cagliari,
Dipartimento di Ingegneria Elettrica ed Elettronica
Piazza D'Armi, 09123 Cagliari, Italy
Email:alfio@diee.unica.it

***Abstract*—In this paper, a torque control algorithm for direct drive wind turbines using a twelve-phase permanent magnet synchronous electrical machine is proposed. An electrical machine oriented to output four independent 3-phase star subsystems have been introduced in order to improve direct drive wind turbine torque control, power generation and reliability. A specific coordinate transformation for multi-phase electrical machine control that allows the independent and decoupled management of each electric three-phase subsystem has been developed. The synthesis and the simulation results of the proposed control algorithm are presented.**

***Index Terms*—Multi-phase electrical machines control, permanent magnet synchronous generator, renewable energy, wind generation, direct-drive wind turbine .**

I. Introduction

The Doubly Fed Induction Generator (DFIG) is the electromechanical conversion system most widely used for wind turbines (WT). It allows a variable speed turbine control using an electronic power converter connected to the rotor winding with a rated power equal or less to roughly 30% of the electrical machine one. Numerous economic analysis, based on the annual energy yield-total cost ratio, have shown DFIG turbines to be the best compromise. Moreover, these turbines are the lightest and most economical available, explaining why they are one of most widely used in commercial WT [1]. On the other hand the cost is not the only factor to be considered when choosing a WT. In particular, reliability and availability are becoming increasingly important, especially for offshore applications. In this framework, the gearbox is one the most critical component [2]. Furthermore, the need to improve voltage fault ride-through capability, power-quality requirements for grid-connection and efficiency, are steering towards a novel transition: the direct drive wind turbine (DDWT) or a hybrid solution with a single-stage gearbox [3] [4].

The characteristics of the DDWT are the direct connection of blade shaft to the electric generator and the use of a full size front-end converter. By avoiding the use of the gearbox, the direct drive configuration reduces both the main conversion system losses and maintenance requirements and also overcomes, due to full size converter grid interface, the problem of voltage disturbances caused by grid faults and voltage dips. However, the use of low-speed high-torque generators and fully rated front-end inverters makes these wind turbines more expensive [1] [3].

Many types of DDWT have been proposed in the technical literature using different kind of electrical machine. The comparison between the PM synchronous machine, induction machine and the switched reluctance machine has highlighted that the PM synchronous machines leads, for a given torque rating, to the lower use of active material mass making it suitable for high power applications [5].

In this paper a radial flux surface mounted permanent-magnet generator with distributed stator winding is examined. In particular, a multi-phase configuration characterized by an internal stator configuration has been analysed.

The main reasons of multi-phase choice for DDWT are the possibility to split the power and the current between a higher number of phases, allowing the per-phase inverter power rating reduction. Furthermore, this configuration guarantees WT working continuity, even in presence of phase and/or inverter faults. Hence, the use of multi-phase electrical machines in DDWT should enable to increase the reliability, the working time and, consequently, the annual energy yield, determining a reduction in the production and maintenance costs [2] [10] [16].

Furthermore, the versatility of multi-phase generators allows: to manage in a more flexible way the WT power production and distribution due to intrinsic higher degree of freedom; to reduce the torque ripple component produced by stator MMF and PM field spatial harmonic interaction; to increase efficiency ; to reduce the effect of DC side voltage ripple due to the frequency reduction. Moreover, if the phase number is odd it is possible to enhance the torque generation by means of stator current harmonic injections. This property can be extended to even numbers of phases in the case of asymmetrical six-phase machine with a single neutral point [10] [11]. Presently the application of multi-phase PM machine to DDWT is limited to small power applications due to design constraints of electrical machine. In fact, the number of pole pairs assumes particulary high values in the DDWT due to the shaft speed reduction. Therefore, the pole pitch dimension enlargement, caused by multi-phase winding distribution, could determine, in presence of high number of phase, an excessive increase of electrical machines rotor size.

The development of AC machines characterized by multi-

978-1-4673-1301-8/12/$31.00 ©2012 IEEE

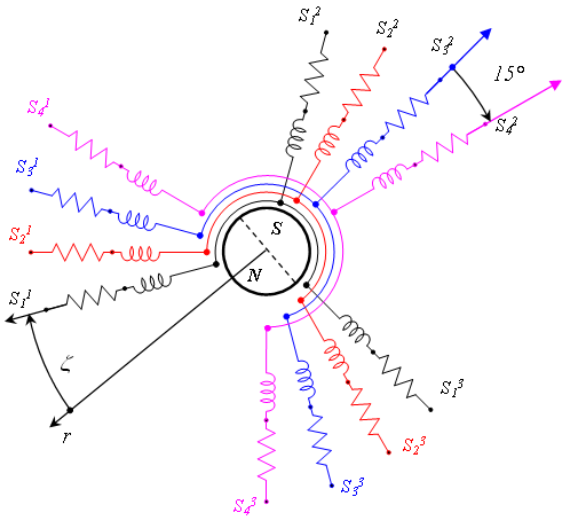

Fig. 1. Schematic of the mechanical structure of a DDWT PM synchronous electrical generator

phase concentrating and fractional slot balanced winding has permitted to overcome some of the design limitations above reported, allowing the realization of low speed WT multiphase PM machines [7] [8] [12].

On the other hand, the multiphase fractional slot electrical machines are still considered special machines with a limited diffusion and operative experience for allowing a rapid and massive implementation on high power DDWT. For this reason, it is believed that the reliability connected to the manufacture experience on high power distributed winding multiphase electrical machines will play an important role in the definition of the time transition between the two technologies.

In this paper, an application of a twelve-phase PM generator characterized by four three star distributed full pitch windings with isolated neutral point for a DDWT application has been investigated. In particular, the modeling and the development of a control algorithm that allows the independent and decoupled management of the four electrical subsystem has been proposed in order to improve the reliability and the efficiency of the wind energy conversion process.

II. Multi-Phase PM Generator Wind Turbine Structure

At the present time the reference WT power rating is $3\,MW$. In DDWT PM generator design the starting point is the frequency specification because the use of a large number of poles affects the electrical machine main dimensions [6]. Referring to typical $3\,MW$ WT parameters, the number of pole pairs p has been set to 150.

In order to split the wind energy production between four identical power systems, a multi star configuration of PM synchronous generator has been set as a system design constraint. As well known the condition of circular symmetry imposes that the spatial displacement between any two consecutive stator phases be equal to $\alpha = 2\,\pi\,/\,m$. However, if the number of phases, m, is an even prime number or an odd number, the stator windings may be distributed asymmetrically.

In the case of odd stator windings, partitioned in three phase sub-systems, the spatial displacement between two consecutive windings sub-systems can be $\alpha = \pi\,/\,m$. When this spacial phases configuration is used each sub-system neutral point has to be kept isolated [10].

The main advantage of this configuration in the case of six phase asymmetrically distributed machines partitioned in two three phase subsystems is that it behaves as a twelve-phase symmetrically distributed PM machines by the electromechanical point of view [10] [12].

Basis on the above design constraint a twelve-phases asymmetrically distributed PM synchronous generator has been defined referring to the preliminary electrical machine design procedure reported in [1] [3]. The parameter of the muti-phase generator is reported in Table I. In Fig.1 a one pole pair schematic representation of the twelve-phase asymmetrically distributed PM machines is reported.

In Fig.2 the schematic representation of the proposed DDWT configuration is presented. Each three phase sub-system is connected to an AC/DC current controlled converter of $2\,kV$ DC rating voltage and of $750\,kV\,A$ power rating connected to a floating point capacitor bank.

This configuration is extremely simple and reliable as it does away the gearbox, the component with the higher failure rate. Moreover, the electronic power converter, one of the most critical components in the DDWT, has been replaced with four smaller ones. This design enhances the reliability and flexibility, while reducing the cost of the WT. Furthermore, the system continues to operate in the event of one inverter failure, even at nominal WT speed, by appropriately controlling the WT blade pitch angle.

This electrical configuration is particularly suitable for offshore applications thanks to the DC output. This allows one to choose, using a specific wind farm distribution configuration and a suitable DC/DC conversion system, the appropriate DC voltage level for the electric power distribution and transmission [13].

TABLE I
12-phase PM Generator Characteristic

Rating Power	P_n	$[\,MW\,]$	3
Rating Voltage	V_n	$[\,kV\,]$	1.5
number of phase	m		12
number of pole pairs	p		150
stator diameter	D	$[m]$	6
air gap	δ	$[mm]$	6
resistivity of copper at $120°C$	ρ_m	$[\mu\Omega\,m]$	0.025
Inductance per phase	L_m	$[mH]$	4
Stator resistance	R_s	$[m\Omega]$	250

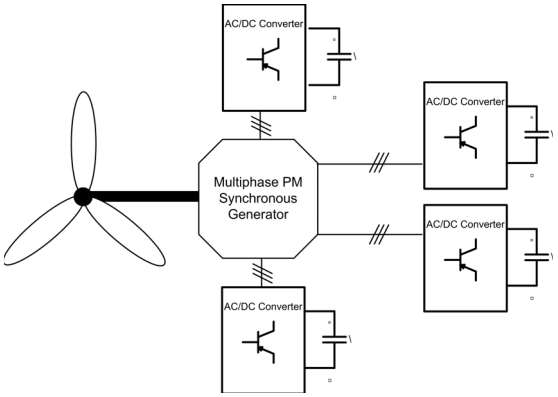

Fig. 2. DDWT schematic representation of the electric configuration used for the power management of the twelve-phases PM synchronous electrical generator

III. Mathematical Model of PM Multi-Phase Generator

In order to develop the control system, the dynamic mathematical model of twelve phase asymmetrical PM synchronous machine has been developed. The saturation effect, the saliency effect, the time temperature parameter dependence and the cogging torque have not been considered in the modeling.

The winding structure and the no sinusoidal space distribution of PM air gap flux density should suggest the development of a modeling procedure that takes into account the effect of higher space harmonic components. However the optimization design procedure of multi-phase PM machine devoted to reduce the effect of torque harmonic ripple allows the use of first space harmonic component is sufficiently exhaustive to represent the dynamic electromechanical behavior of multi-phase machine [14].

The transformation matrices generally used for asymmetrical multi-phase machines are based on the generalization of Clarke's or Park's ones.

The stator voltage $\overline{v}^s$, current $\overline{i}^s$ and stator flux $\overline{\lambda}^s$ vectors referred to the stator reference frame, are represented by the twelve component vectors reported in Eq.(1), where the subscript represents the phase and the apex the respective three-phase sub-system index.

$$\begin{array}{rcl} \overline{v}^s & = & \left[v_a^1, v_b^1, v_c^1, \cdots v_a^k, v_b^k, v_c^k \cdots v_a^4, v_b^4, v_c^4\right]^T \\ \overline{i}^s & = & \left[i_a^1, i_b^1, i_c^1, \cdots i_a^k, i_b^k, i_c^k \cdots i_a^4, i_b^4, i_c^4\right]^T \\ \overline{\lambda}^s & = & \left[\lambda_a^1, \lambda_b^1, \lambda_c^1, \cdots \lambda_a^k, \lambda_b^k, \lambda_c^k \cdots \lambda_a^4, \lambda_b^4, \lambda_c^4\right]^T \end{array} \quad (1)$$

Using this formalization, the stator voltage equation assumes the form reported in Eq.(2) where R_s is the phase stator resistance and $\mathbf{I}^{12}$ is the twelfth order identity matrix.

$$\overline{v}^s = R_s\, \mathbf{I}^{12} \cdot \overline{i}^s + \frac{d\,\overline{\lambda}^s}{d\,t} \quad (2)$$

Referring to Fig.1 and expressing with n the number of three-phase subsystems, with f the phase number of each sub-system ($a = 1$, $b = 2$, $c = 3$) and ϑ the instantaneous electrical angular position of PM rotor flux vector reference frame with respect to stator one; the stator flux vector components λ_f^k can be expressed by Eq.(3) where λ_m is the maximum value of the single phase flux associated to the rotor Permanent Magnet and β_f^k is the electrical displacement angle of the considered phase with respect to the reference one.

$L_{f\cdot k,j}^s$ is the general representation of mutual and self stator phase inductance whose value is expressed by the Eq.(4) where s is the superior natural integer of the ratio j/n. The element $L_{i,j}$ is the component of the inductance matrix $\mathbf{L}$ of multiphase electrical machines. These last two equations describe the magnetic coupling between the twelve electrical circuits and assume a particular relevance in the present model.

$$\lambda_f^k = \sum_{j=1}^{m} L_{f+k-1,j}^s \cdot i_j^s + \lambda_m\, e^{j\left(\vartheta+\beta_f^k\right)} \quad (3)$$

$$\begin{array}{l} L_{i,j}^s = L_{dm} \cdot \cos\left[\frac{\pi}{m}\,(j-1) + \frac{\pi}{3}\,(s-1) - \frac{\pi}{m}\,(i-1)\right] + \\ + L_{sd}\,\delta_{i,j}; \qquad s = SI(\frac{j}{n}) \end{array} \quad (4)$$

A Park transformation, $\mathbf{P}$, for the case of twelve phase asymmetrically spatial distributed PM electrical machine, reported in Eq.(5), has been used to obtain the dqo representation of the analyzed twelve phase PM generator.

$$\begin{array}{l} P = \kappa\,\left[\,p_{i,j}\,\right]^{12X12} = \\ = \left\{ \begin{array}{ll} p_{k,nf+c} & = cos\left[\vartheta + f\,\frac{2\,\pi}{3} + \frac{\pi}{3\cdot n}(k-1)\right] \\ p_{n+k,nf+k} & = sin\left[\vartheta + f\,\frac{2\,\pi}{3} + \frac{\pi}{3\cdot n}(k-1)\right] \\ p_{2n+k,nf+k} & = \frac{1}{2} \\ 0 \;\; elsewhere & k \in [1 \cdots n] \end{array} \right. \end{array} \quad (5)$$

The application of Park transformation $\mathbf{P}$ to Eq.(2) allows the representation of each three phase sub system in dqo reference frame; in this case the electrical machine model assumes the form reported in Eq.(6).

$$\overline{v}_{dqo}^k = R_s\,\overline{i}_{dqo}^k + \jmath\,\omega_r\,\overline{\lambda}_{dqo}^k + \frac{d\,\overline{\lambda}_{dqo}^k}{d\,t} \quad (6)$$

The results of Park's application to inductance matrix $\mathbf{L}$ is reported in Eq.(7)

$$\mathbf{L}_{dqo} = \left[\begin{array}{ccc} [L_d]^{4\times 4} & [0]^{4\times 4} & [0]^{4\times 4} \\ [0]^{4\times 4} & [L_q]^{4\times 4} & [0]^{4\times 4} \\ [0]^{4\times 4} & [0]^{4\times 4} & [L_o]^{4\times 4} \end{array}\right] \quad (7)$$

In particular, when the windings are connected in order to form n three phase subsystems with isolated neutral point, the zero sequence components can be neglected reducing the number of equations and variables [10]. Moreover, under the hypothesis of linear operating conditions, each three-phase subsystem can be described in $d-q$ axis and the multi-phase machine model can be obtained as a set of $d-q$ equations in which the

torque is given by the sum of each three-phase subsystem contributions [9] [10].
In the present paper this model approach has been used. In particular, being the electrical machine characterised by a magnetic isotropy, the value of L_q is equal to L_d.
In the PM rotor flux vector reference frame, the stator flux vector $\overline{\lambda}_{dq}^{k}$ can be expressed as in Eq.(8)

$$\overline{\lambda}_{dq}^{k} = \lambda_m + \frac{3}{2} L_m \sum_{j=1}^{4} \bar{i}_{dq}^{j} + L_{ls}\, \bar{i}_{dq}^{k} \tag{8}$$

The dq-voltage equation of the k-th subsystem can be expressed also referring to the base frequency in the form reported in Eq.(9),

$$\overline{v}_{dq}^{k} = R\,\mathbf{I}^2\, \bar{i}_{dq}^{k} + j\,\frac{\omega_r}{\omega_b}\,\overline{\psi}_{dq}^{k} + \frac{1}{\omega_b}\,\frac{d\,\overline{\psi}_{dq}^{k}}{d\,t} \tag{9}$$

where the relation between the flux per second $\overline{\psi}_{dq}^{k}$ and current vectors assumes the form reported in Eq.(10) being X_m and X_{ls} respectively the linkage and the leakage reactance referred to the base frequency.

$$\overline{\psi}_{dq}^{k} = \psi_m + \frac{3}{2} X_m \sum_{j=1}^{4} \bar{i}_{dq}^{j} + X_{ls}\, \bar{i}_{dq}^{k} \tag{10}$$

The flux per second vector $\overline{\psi}_{dq}^{k}$ of k-th sub-system shows that the mathematical model of twelve-phase PM generator is fair complex also after the Park transformation. Moreover, the space vector voltage equation reported in Eq.(11) of the k-th three phase system highlights the presence of the coupling between all sub-systems, which introduces a high degree of complexity in the application of the classical linearization procedure for the current vector control synthesis.

$$\begin{aligned}\overline{v}^{k} \;&= R\,\bar{i}^{k} + j\,\tfrac{\omega_r}{\omega_b}\left[\psi_m + \tfrac{3}{2}\,X_m \sum_{j=1}^{n} \bar{i}^{j} + X_{ls}\,\bar{i}^{k}\right] + \\ &+ \tfrac{3}{2}\,\tfrac{X_m}{\omega_b} \sum_{j=1}^{n} \frac{d\,\bar{i}^{j}}{dt} + \frac{X_{ls}}{\omega_b}\,\frac{d\,\bar{i}^{k}}{dt}\end{aligned} \tag{11}$$

In accordance with the mathematical model, the torque equation for this type of electrical machine assumes the form reported in Eq.(12)

$$T_e = p\,\lambda_m \sum_{j=1}^{n} i_q^{j} = p\,\frac{\psi_m}{\omega_b} \sum_{j=1}^{n} i_q^{j} \tag{12}$$

IV. Decoupling Control of PM Multi-Phase Generator

In order to determine a transformation that allows the extention of the classical methodology for synthesis and implementations of current vector control to multi-phase PM electrical machines, a holistic mathematical description of the system has been developed. A complex vector representation characterized by the use of complex elements of stator voltage $\dot{\overline{\mathbf{v}}}$, stator current $\dot{\overline{\mathbf{i}}}$ and permanent magnet flux induced voltage $\dot{\overline{\Psi}}_M$ has been introduced:

$$\begin{aligned}\dot{\overline{\mathbf{v}}} &= \begin{bmatrix}\overline{v}_1 & \dots & \overline{v}_n\end{bmatrix}^T \\ \dot{\overline{\mathbf{i}}} &= \begin{bmatrix}\bar{i}_1 & \dots & \bar{i}_n\end{bmatrix}^T \\ \dot{\overline{\Psi}}_M &= \begin{bmatrix} j\frac{\omega_r}{\omega_b}\,\overline{\psi}_m & \dots & j\frac{\omega_r}{\omega_b}\,\overline{\psi}_m\end{bmatrix}^T\end{aligned} \tag{13}$$

Using the above quantities and referring to Eq.(11), the voltage equation of the multi-phase PM Generator can be expressed in the following form:

$$\dot{\overline{\mathbf{v}}} = \dot{A}\,\dot{\overline{\mathbf{i}}} + \dot{\overline{\Psi}}_M = \left(\dot{A}_{ls} + \dot{A}_m\right)\,\dot{\overline{\mathbf{i}}} + \dot{\overline{\Psi}}_M \tag{14}$$

The complex matrix, $\dot{A}$ can be spitted into the sum $\dot{A}_{ls}$ and $\dot{A}_m$ ones. The $\dot{A}_{ls}$ is $n \times n$ complex diagonal matrix characterized by elements all equal to $\dot{a}_{ls}$ which expression is reported in the following:

$$\dot{a}_{ls} = R + \frac{X_{ls}}{\omega_b}\,\wp + j\,\frac{\omega_r}{\omega_b}\,X_{ls} \tag{15}$$

and where $\wp$ represents the time derivative operator. The $\dot{A}_m$ is a $n \times n$ complex square matrix characterized by elements all equal to a_m reported in the Eq.(16).

$$a_m = \frac{3}{2}\,\frac{X_m}{\omega_b}\,p + j\frac{3}{2}\,\frac{\omega_r}{\omega_b}\,X_m \tag{16}$$

The application of the Jordan decomposition allows the achievement of the space transformation that, in turn, leads to the $\dot{A}$ matrix diagonalization. The result, reported in Eq.(17), is the definition of a novel model of PM multiphase electrical machines that permits to define clearly the terms for the implementation of decoupling and feed-forward actions. In fact, introducing the modeling, described in the relations (18), the space transformation that simplifies and decouples the control of the multi-phase PM Generator can be obtained. Considering the matrix Q of Eq.(17) and its inverse:

$$Q = \begin{bmatrix} 1 & 1 & 0 & 0 \\ 1 & 0 & 1 & 0 \\ 1 & 0 & 0 & 1 \\ 1 & -1 & -1 & -1 \end{bmatrix} \tag{17}$$

and introducing the following transformation:

$$\begin{aligned}\dot{\overline{\mathbf{v}}}_J &= Q^{-1}\,\dot{\overline{\mathbf{v}}} \\ \dot{\overline{\mathbf{i}}}_J &= Q^{-1}\,\dot{\overline{\mathbf{i}}} \\ \dot{\overline{\Psi}}_{MJ} &= Q^{-1}\,\dot{\overline{\Psi}}_M\end{aligned} \tag{18}$$

the voltage equation assume the form reported in Eq.(19)

$$\dot{\overline{\mathbf{v}}}_J = Q^{-1}\,\dot{A}\,Q\,\dot{\overline{\mathbf{i}}}_J + \dot{\overline{\Psi}}_{MJ} = \dot{D}\dot{\overline{\mathbf{i}}}_J + \dot{\overline{\Psi}}_{MJ} \tag{19}$$

where $\dot{D}$ is a complex diagonal matrix that can be split into its real and imaginary part, denoted by $\dot{D}_1$ and $\dot{D}_2$ respectively. $\dot{\overline{\Psi}}_{MJ}$ assumes the form reported in Eq.(20)

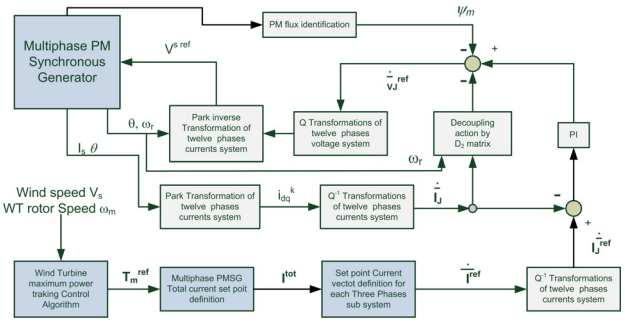

Fig. 3. Block diagram of proposed DDWT control scheme

$$\dot{\bar{\Psi}}_{MJ} = \left[\jmath \frac{\omega_r}{\omega_b} \bar{\psi}_m \, 0 \cdots 0 \right]^T \tag{20}$$

The use of the proposed transformation allows the simplification of the model of twelve phase PM machines transforming the four vector equations in a form in which it is clearly and easily defined the motion decoupling term and the PM induced voltage is applied just in the first of the four equivalent circuits and, hence, can be directly canceled by means a feed-forward action if the permanent magnet flux induced voltage is known. The proposed transformation has been used to develop a stator current vector control.

A. Current control

To achieve a torque a control, the stator current vector control of each three-phase system has been implemented. Referring to Eq.(19) the current equation can be expressed in the canonical form shown in Eq.(21)

$$\dot{\bar{x}} = A\bar{x} + B\bar{u} \tag{21}$$

where $\bar{x} = \bar{\mathbf{i}}_J$. Using this representation the feed-forward and decoupling control action can be evidenced in a straightforward manner and PI current loop controllers synthesized by implementing an internal mode control [15] . The current control scheme for the machine as a whole is shown in Fig.3 and the PI parameter of the first loop referred to the first row element of $\dot{D}_1$ matrix takes the value reported in Eq.(22)

$$\left| \begin{array}{rcl} k_P^1 & = & \alpha_c \frac{X'}{\omega_b} \\ k_I^1 & = & \alpha_c R \end{array} \right. \tag{22}$$

where $X' = 6\,X_m + X_{ls}$ and the other values are reported in Eq.(23)

$$\left| \begin{array}{rcl} k_P & = & \alpha_c \frac{X_{ls}}{\omega_b} \\ k_I & = & \alpha_c R \end{array} \right. \tag{23}$$

where α_c is the desired closed-loop bandwidth of the current loop.

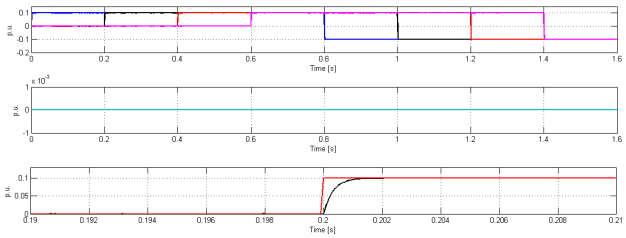

Fig. 4. a) i_q time evolutions b) i_d time evolutions c)zoom on transient evolution of i_q and set-point components

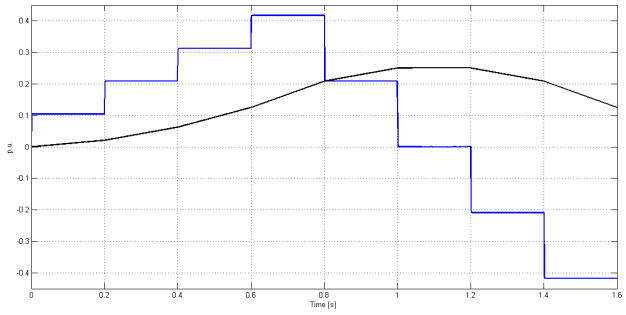

Fig. 5. Torque Speed time evolution in presence of PM sinusoidal EMF

B. Simulation results of proposed multi-phase current control

The current control of $3MW$ twelve-phase permanent magnet synchronous electrical machine has been simulated by using the Matlab-Simulink software. The main parameters of the electrical machine are reported in Table I. The PI current loop controllers are synthesized imposing a bandwidth of $500\,Hz$. In order to evaluate the performance of the proposed control algorithm, a simulation of the permanent magnet synchronous electrical machine under the hypothesis of sinusoidal spatial distribution of air gap PM field has been firstly carried out imposing a sequential connection of each electrical sub-systems with a $200\,ms$ time interval characterized by the application of i_q steps set-point of 0.1 p.u. for each sub-system. An inversion in the torque set-point of each sub-system has been applied with the aim of verifying the independent torque control that can be developed by each sub-system.

In Fig.4 is reported the time evolution of reference and actual i_q and i_d currents in each sub-system. The zoom on the second sub-system i_q transient current evolution shows the good matching between the actual and the designed bandwidth. Moreover, the analysis of the i_d components highlights the goodness of the decoupling action developed by the proposed coordinate transformation and points out the absence of interaction between the d and q components of different subsystem.

In Fig.5 is reported the torque and speed time evolution in correspondence to the iq components evolution.

To analyze the effect higher spatial harmonic PM field distribution, a PM spatial configuration capable to generate the

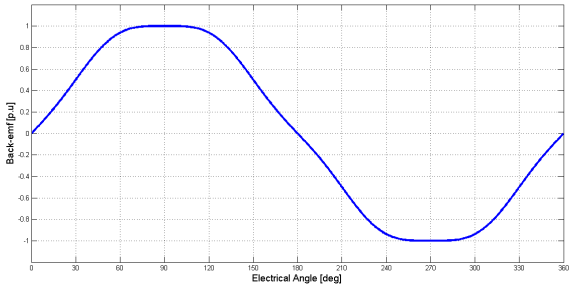

Fig. 6. EMF generated on a single phase by PM flux at rated speed

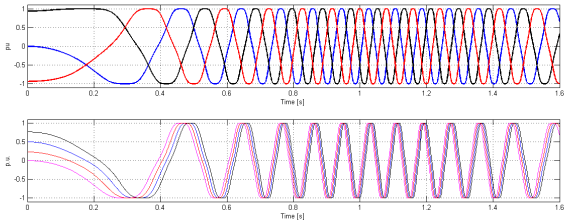

Fig. 7. a) time evolution of PM flux in the stator winding of the first sub-system b) time evolution of PM flux in the first phase of each sub-system

phase back-emf waveform at rated speed reported in Figure 6 has been modeled and used to perform the same simulation above described.

The results are reported from Fig.7 to Fig.11.

In Fig.7 is reported the evolution of PM flux time evolution in the first sub-system and in the first phase of each sub-system. The effect of the fifth spatial harmonic determines the presence of higher time harmonic in the PM flux that determine the introduction of fluctuation of its d and q components on each sub-system, as can be observed in Fig.8. The principal effect of the PM higher harmonic can be observed in Fig.11 where a torque ripple occurs when an odd number of sub-systems are fed. On the contrary when the powered sub-system are displaced by 30 electrical degree, the torque ripple is zero, confirming the results reported in the scientific literature for this kind of multiphase machine [12]. The time evolution of both i_q and i_d currents, reported in Fig.8, and those of AC stator currents in the first phase of each subsystem, reported in Fig.10, points out that the proposed control algorithm guarantees the decoupling action also in presence of PM non sinusoidal spatial distribution.

The simulation results highlight the improvement obtained and confirm the opportunity to use this control configuration for DDWT application. In fact, the possibility to reduce the torque ripple is an important element to cut the effect due to the structural mechanical stress produced by torque ripple on the blade and on the wind turbine mechanical system.

V. Conclusion

In this paper, a twelve-phase permanent magnet synchronous electrical machine for direct direct drive for direct drive wind turbine is proposed. In particular, a novel specific

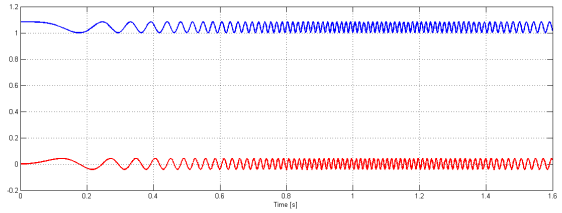

Fig. 8. d-q components time evolution of PM flux in the first sub-system

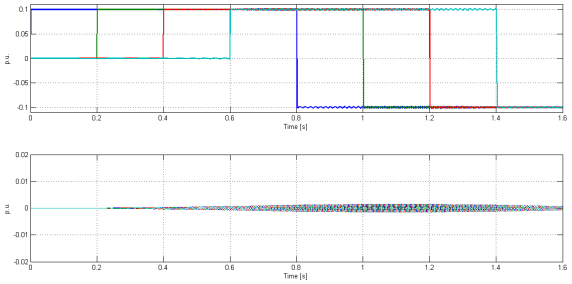

Fig. 9. a) q sub-system stator current time evolution b) q sub-system stator current time evolution

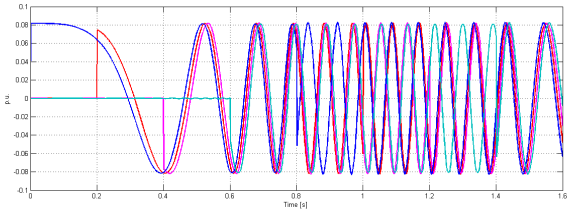

Fig. 10. Stator current in the fist phase of each sub-system of PM multiphase machine

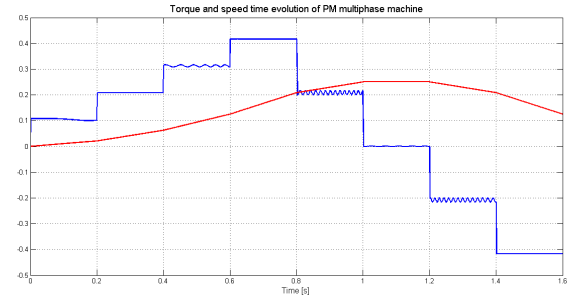

Fig. 11. Torque Speed time evolution in presence of non sinusoidal PM EMF

coordinate transformation for multi-phase electrical system has been introduced in order to develop a torque control algorithm devoted to multi phase application and characterized by an indipendent and decoupled current control. The sysntesis and the mathematical modelling of the proposed control algorithm have been reported. The simulation referred to a sinusoidal and non sinusoidal PM induction distibution have been developed. The results obtained highlight the validity of the proposed control tecnique.

REFERENCES

[1] H. Polinder, F. F. A. van der Pijl, G. de Vilder, and P. J. Tavner, "Comparison of Direct-Drive and Geared Generator Concepts for Wind Turbines", *IEEE Trans. on Energy Conversion*, Vol. 21, NO. 3, September 2006

[2] J. Ribrant and L. M. Bertling, "Survey of Failures in Wind Power Systems With Focus on Swedish Wind Power Plants During 1997-2005" *IEEE Trans. on Energy Conversion*, Vol. 22, No. 1, March 2007

[3] Yu-Shi Xue, Li Han, Hui Li, Li-Dan Xie; "Optimal Design and Comparison of Different PM Synchronous Generator Systems for Wind Turbines" *Proc. of International Conference on Electrical Machines and Systems-ICEMS 2008* Wuhan, China, 17-20 Oct. 2008, Page(s): 2448 - 2453

[4] Z. Chen, and E. Spooner, Senior Member, "IEEE Grid Power Quality with Variable Speed Wind Turbines", *IEEE Trans. on Energy Conversion*, Vol.16, n.2, June 2001

[5] M. R. J. Dubois, "Optimized Permanent Magnet Generator Topologies for Direct-Drive Wind Turbines" *Ph.D. dissertation*, Technische Universiteit Delft, Netherland, 2004

[6] Yicheng Chen, P. Pillay, A. Khan; "PM wind generator topologies" *IEEE Trans. on Ind. Appl.*, Volume: 41 , Issue: 6 Year: 2005 , pp:1619 - 1626.

[7] A.M. EL-Refaie,"Fractional-Slot Concentrated-Windings Synchronous Permanent Magnet Machines: Opportunities and Challenges" IEEE Trans. Ind. Electr., vol.57, n.1, Jan. 2010

[8] D. Vizireanu, S. Brisset, and P. Brochet, "Design and optimization of a 9-phase axial-flux PMsynchronous generator with concentrated winding for direct-drive wind turbine",*Proc. of IEEE IAS Annu. Meeting*, Tampa, FL, 2006, pp.1912-1918.

[9] T. A. Lipo, "A d-q model for six phase induction machines",*Proc. Int. Conf. Electrical Machines (ICEM)*, Athens, Greece, 1980, pp. 860-867.

[10] E. Levi, "Multiphase Electric Machines for Variable-Speed Applications" *IEEE Trans. Ind. Electr.*, Vol.55, n. 5, may 2008.

[11] X. Kestelyn, E. Semail, "A vectorial Approach for Generation of Optimal Current Refernce for Multiphase Permanent Magnet Syncrhronous MAchines in Real Time" *IEEE Trans. Ind. Electr.* vol.58,n.11 nov. 2011, pp:5057-5065

[12] E. Semail, F. Scuiller, J.F. Charpentier, "Charpentier Multi-star multiphase winding for a high power naval propulsion machine with low ripple torques and high fault tolerant ability". *Proc. IEEE Conference on Vehicle Power and Propulsion (VPPC)*, Year: 2010 , Page(s): 1 - 5

[13] C. Meyer, M. Hoing, A. Peterson, R. W. De Doncker, "Control and Design of DC Grids for Offshore Wind Farms", *IEEE Trans.on Ind. Appl.*, Vol. 43, no. 6, pp. 1475-1482 November/December 2007.

[14] J. Figueroa, J. Coros, F. Viarogue, "Generalised Transformation for Polyphase Phase MOdulation Motors" *IEEE Trans. on Energy Conversion* vol.21, n.2, June 2006, pp. 332-341.

[15] L. Harnefors, H. P. Nee, "Model-based current control of AC machines using the interna model control method", *IEEE Trans. Ind. Appl.* vol.34,n.1 pp.133-141, Jan.-Feb 1998

[16] D. Vizireanu, S. Brisset, X. Kestelyn, P. Borchet, Y. Milet, and D. Laloy, "Investigation on multi-star structures for large power direct-drive wind generator", *IEEE Trans. Electr. Power Compon. Syst.*, vol. 35, no. 2, pp. 135-152, 2007